Absorption of Organic Compounds by Mesoporous Silica Discoids

Shajesh Palantavida^{1, 1}, Berney Peng², Igor Sokolov^{1,2,3,*}

Abstract: Multiple organic compounds pose a threat to human health. Here we report on the synthesis of a novel nanostructured absorbent, mesoporous colloidal silica particles (pore size of ~3nm, surface are >1100 m²/g, discoid-shaped microns in size) that can be an effective sorbent for organic compounds due to their large surface area. The particle surface is hydrophobized through a trimethylchlorosilane treatment, which was controlled on the level of bulk (TGA analysis) and single particles (confocal Raman spectroscopy). We present the results of the study of the sorption of ten organic compounds of various molecular size and polarity. It is found that our particles can absorb some organic compounds from water up to more than 100% by weight. No substantial dependence of the sorption efficiency on the molecular size was found. Despite a complex nanoscale environment, it was found that the sorption efficiency inversely correlates with the polarity of the organic components, which is similar to the classical sorbents. Further, we demonstrate a strong correlation between the presence of hydrophobic groups and the absorbed compound with a submicron resolution by means of confocal Raman microscopy. This knowledge can be used to design new efficient absorbents.

¹ Department of Mechanical Engineering, Tufts University, 200 College ave., Medford, MA 02155, USA;

² Department of Biomedical Engineering, Tufts University, 547 Boston ave., Medford, MA 02155, USA.

³ Department of Physics, Department of Physics, Tufts University, 547 Boston ave., Medford, MA 02155, USA.

¹ Present address: Center for Nano and Material Sciences, Jain University, Jakkasandra, Kanakapura, Karnataka 562112 India.

^{*} Corresponding author. Department of Mechanical Engineering, Tufts University, 200 College ave., Medford, MA 02155, USA; tel: 1-617-627-2548; igor.sokolov@tufts.edu

KEYWORDS: nanoporous silica; mesoporous silica colloids; organic and oil adsorption; solgel self-assembly; Raman spectroscopy

1. Introduction

Oil spills and other organic contaminations are quite common and pose a substantial threat to human health and the environment. Recently synthetic organic materials have been introduced for the removal of organic contaminants. Use of mesoporous polymer gels [1, 2], polymer fibers [3, 4], polymer/silica composites [5-8], resins [9], polymer and natural fiber foams [10-13] have been reported. The main advantage of such materials is their inherent hydrophobicity/oleophilicity, which is required for the effective absorption of organic compounds. Oil-absorbing inorganic materials include naturally occurring clay minerals [14] and synthetic porous materials [15-18]. Polymer coated iron oxide particles have recently emerged as convenient absorbents since they can be manipulated with a magnetic field [19, 20]. Metal-organic frameworks are relatively new materials studied for oil/water separation [21, 22]. Hydrophobic aerogels have conventionally been explored for oil adsorption/absorption applications [23-25]. In recent years carbon-based materials have gained prominence for oil absorption in the aerogel form [26], though recent advances have been fueled by composites of organic and inorganic absorbents [27]. The major advantage of inorganic absorbents over organic absorbents would be their chemical inertness, resistance to fouling, eco-friendliness, and extensive reusability. In this scenario, silica-based porous absorbents are an environmentally benign and economically viable alternative.

Ordered mesoporous materials (OMM) form a unique class of materials due to their engineered porosity. It finds applications in diverse fields ranging from sensors, catalysts, adsorbents and absorbents, molecular sieves, energy materials, drug delivery vehicles and so on [28-33]. Silica is undoubtedly the most versatile and most investigated material for OMM by virtue of the high degree of chemical control possible for its precursors, ease of modification of surface functionalities, and high stability of resulting hierarchical structures [34-37]. A high surface to volume ratio, the surface area comparable to zeolites and aerogels, and easily modifiable surface make these materials well-suited for sorption applications. Functionalized OMMs have been demonstrated as absorbents of organic pollutants, heavy metals [38], and carbon dioxide [39-41].

The absorption of gasoline and hexane on hydrophobized SBA-15 materials was studied in [42]. The observed performance was comparable to the best commercial absorbents. Comparing the performance of OMM and carbon absorbents, the mesoporosity reduced internal mass transfer resistance, which facilitated fast adsorption kinetics [43]. Hydrophobicity of the surface improved adsorption capacity and ease of diffusion aided regeneration of the absorbed molecules [44]. The effects of silvlation of OMMs on the absorption of volatile organic compounds was investigated in [45]. It was observed that hydrophobized OMMs always favor the absorption of the organic compound when in competition with water. Furthermore, such OMMs outperform zeolites in absorption capacity when sorbing molecules that have the same polarity. In another work, hydrophobization was achieved through co-condensation of silica precursors, and specific interaction of the adsorbed molecules with the surface modification was observed [46]. Favorable effects of hydrophobization of OMMs on the absorption capacity of organic compounds have been widely observed [47, 48]. The absorption of polyaromatic compounds by MCM 41 have been studied recently [49-51]. Cation modified MCM materials have also been investigated for the adsorption and removal of phenyl sulfide and other organic compounds [52, 53]. Amine modification of MCM, using aminopropyl silane has been used to facilitate removal of dye contaminants [54]. Composites of MCM and graphene derivatives have been reported for the removal of organic drugs [55]. Interestingly there are only a few reports on the use of OMMs in the remediation of water contaminated by oil and organic chemical spillages. The aforementioned advantages of OMMs should make them good candidates for the extraction of organic contaminants from water [56, 57].

Previously we have reported on a unique architecture obtained by a templated silica self-assembly, the discoids formed by surfactant assisted-templating [58-60]. Organic silica precursor (tetraethoxysilane) was allowed to undergo hydrolysis and condensation in the presence of CTAB surfactant to obtain the particles. The particles have a high surface area of the order of 1100 m²/g as compared to 800 m²/g observed for most clays [61]. However, the cost of templated mesoporous silica materials obtained is typically prohibitively high for its broad commercial use. The robustness of the synthesis was further demonstrated by using the more 'industry-friendly' inorganic silica precursor, sodium silicate [58, 59]. Inorganic silica precursors have attracted interest as a sustainable and more amiable silica source owing to their lower cost, stability, and

toxicity compared to alkoxide precursors [62]. This also makes them attractive for industrial scaleup.

Here we present mesoporous discoid silica particles obtained from an inorganic silica source, sodium silicate, and hydrophobized by using trimethylchlorosilane. We report on the results on the absorption of organic compounds by these particles by using a diverse set of organic pollutants: chloroform, ethylene glycol, acetonitrile, acetone, dimethylsulfoxide, ethyl acetate, toluene, xylene, 2-butoxyethanol, and ASTM D5307 crude oil standard. Besides standard methods of particle characterization, we present a direct submicron visualization of hydrophobic modification and absorbed organics in the particles' pores using confocal Raman spectroscopy. The obtained results can be used for future design of novel nanostructured absorbents.

2. Experimental

2.1. Materials

Sodium metasilicate nonahydrate (Na₂SiO₃. 9H2O) was obtained from Fischer Scientific. Trimethylchlorosilane and cetyltrimethylammonium bromide (CTAB) was purchased from Aldrich. Hydrochloric acid (HCl) was procured from J T Baker. The solvents chloroform, ethylene glycol, acetonitrile, ethyl acetate, and xylene were obtained from Aldrich. Acetone, toluene, and dimethylsulfoxide were obtained from Fischer. 2-butoxyethanol was obtained from Dow chemicals. All chemicals were used without further purification.

2.2. Synthesis

Mesoporous silica discoids were synthesized using sodium metasilicate nonahydrate as a silica source, cetyltrimethylammonium bromide as a template, and hydrochloric acid (HCl) as a catalyst in the following molar composition: 1 Na₂SiO₃.9H₂O: 1.5 CTAB: 28 HCl: 729 H₂O. In a typical synthesis, 1.6 g of Na₂SiO₃. 9H₂O was dissolved in 55.2 g H₂O stirring for 15 minutes. Separately, 16 g of concentrated HCl was slowly added to 11.2 g CTAB and stirred for 2 min. The clear sodium silicate solution was then slowly added to CTAB/HCl solution and stirred for 5 min. The resulting solution was maintained at room temperature for 24 h under quiescent conditions. The product was

recovered by centrifugation, washed several times with distilled water, and subsequently dried at 70 °C for 2 h. The as-synthesized discoids were calcined at 450 °C in a flowing air atmosphere. Calcined discoids were hydrophobized as follows. The calcined discoids were suspended in 80% trimethylchlorosilane in ethanol (0.25g in 10 ml) for 24 hours. After 24 hours, the solution was decanted and the particles washed thoroughly with ethanol. The washed discoids were then vacuum-dried at 120 °C overnight. The dried powder was used for absorption experiments.

2.3. Characterization, Sorption, and Analysis

Calcined discoids were characterized by N₂ adsorption/desorption isotherms of calcined mesoporous silica samples measured at 77 K on an ASAP 2020 Porosimetry Analyzer (Micromoretics). Before the measurement, samples were degassed at 350 °C for 4 h. Thermogravimetric analysis (TGA) of hydrophobized discoids and discoids with absorbed organic compounds was performed on a Perkin Elmer Thermogravimetric Pyris 1 analyzer. Electron microscopy techniques, SEM (Phenom, FEI) and TEM (JEOL ARM STEM) were used. Raman confocal images were obtained using a confocal Raman microscope Alpha 300 (WITec, Inc.).

The absorption measurements were performed as follows. A 10 ml 20 % solution of the respective compound in water was prepared. Water immiscible compounds were ultrasonicated with stirring to prepare an emulsion. 10 mg of discoids were added to the solution and mixed using a magnetic stirrer for 2h (or less for the kinetic verification experiments). The organic absorbed powder was recovered by air forced filtration. The powder was used for TGA analysis.

3. Results and discussion

SEM images of calcined discoids before and after hydrophobization are provided in Figure 1. One can see no significant change in the microstructure after hydrophobization. TEM images (Fig.1C) show cylindrical nanochannels inside discoids, which are typical for this kind of particles [59, 60].

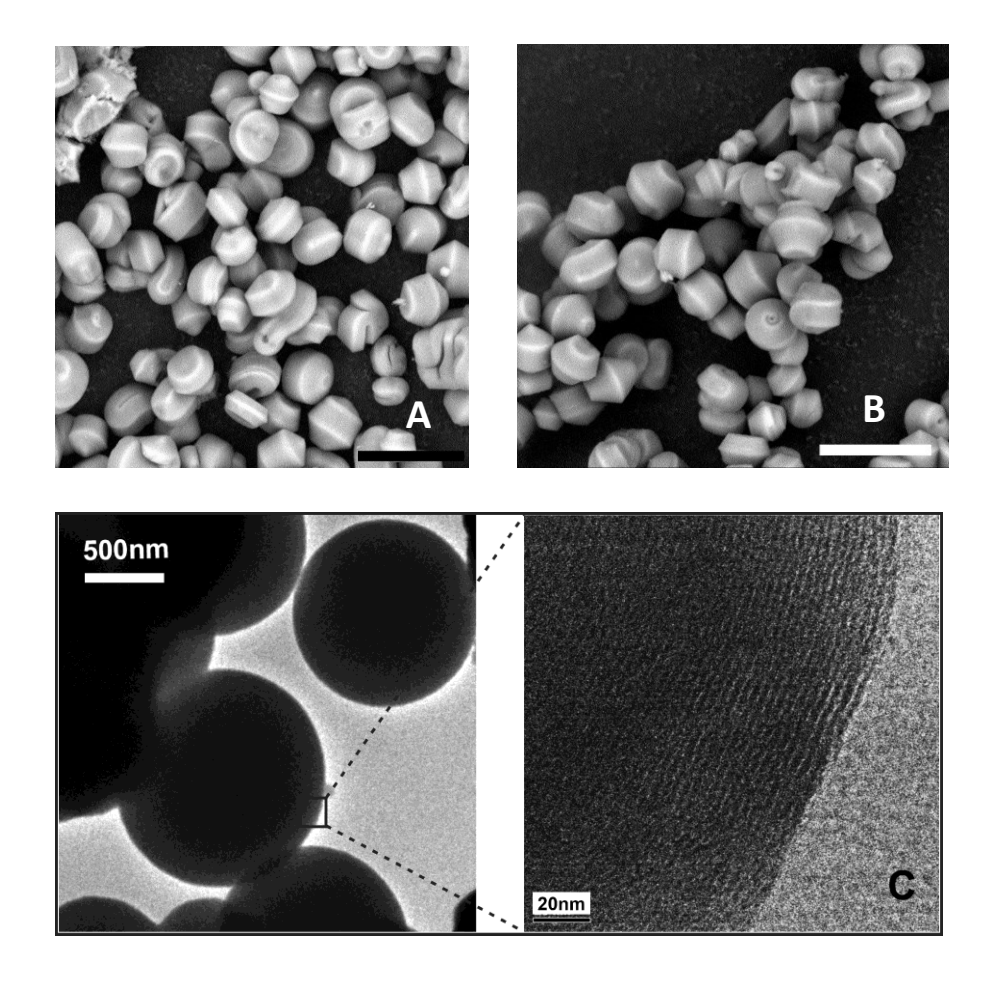


Fig. 1. Electron microscopy images of discoids SEM (A) before and (B) after functionalization. Scale bars are $10~\mu m$; (C) TEM images showing cylindrical nanochannels inside discoids.

The adsorption isotherms of calcined discoids are shown in Figure 2. These isotherms are type IV with a narrow hysteresis loop, which indicates the presence of smooth uniformly sized pores. Such isotherms are typical for ordered mesoporous materials. The BET surface area was found to be 1160 m²/g, and the BJH adsorption total pore volume was 0.84 cm³/g. The average pore diameter was 2.9 nm, which is in agreement with the periodicity seen in Fig.1C. These are typical of CTAB templated ordered mesoporous materials. The nature of porosity in these materials has been investigated in detail in our previous reports [58, 63]. Briefly, the particles are created in the templated sol-gel process of self-assembly. The particle porosity is inherited from the nematic liquid crystal formed by template surfactant molecules. After calcination, the particles possess the same symmetry of the pore structure as the nematic liquid crystal [63, 64], which is hexagonal packaging of cylindrical channels running in parallel.

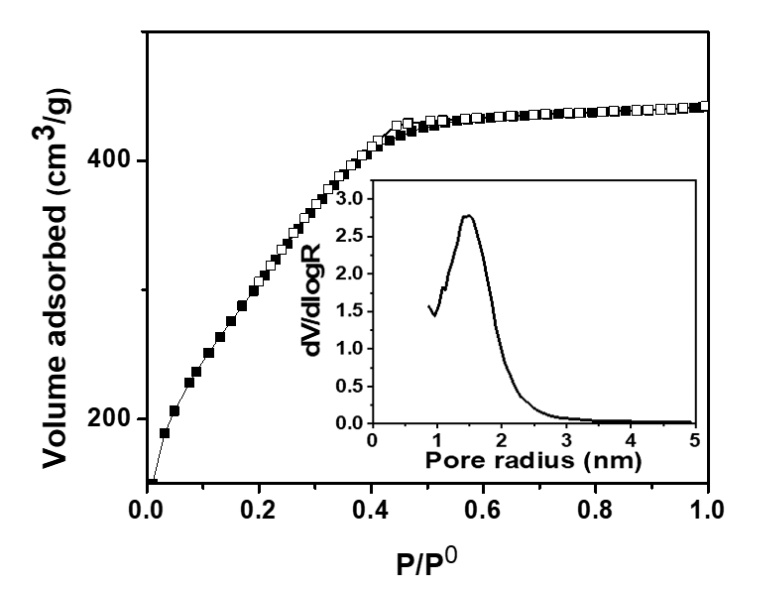


Fig. 2. N₂ adsorption isotherm of calcined discoids (adsorption (solid) and desorption (hollow)). The insert shows the distribution of the pore radius of the discoids.

The extent of the particle modification by hydrophobization could be obtained from the thermal analysis. Figure 3 shows the results of the thermogravimetric analysis. A total weight loss of 7.3 % was observed in the region of 250-1000°C (Figure 3A). One can see three distinctive weight losses using the derivative curve (Figure 3B). The decomposition of chlorosilane modified silica is usually observed about 300-500 °C region. The weight loss of about 300 °C, which is known to be the decomposition temperature of bound surface methyl groups was 2.95 %. Assuming all weight loss is from removing methyl groups (the only unstable organics at these temperatures), one can find that it corresponds to about one methyl group per nm², see the supplementary materials for detail (Table S1). The theoretical surface coverage of methyl groups is reported to be 0.5 nm² per group [61]. It makes the observed coverage equal to half of the theoretical limit.

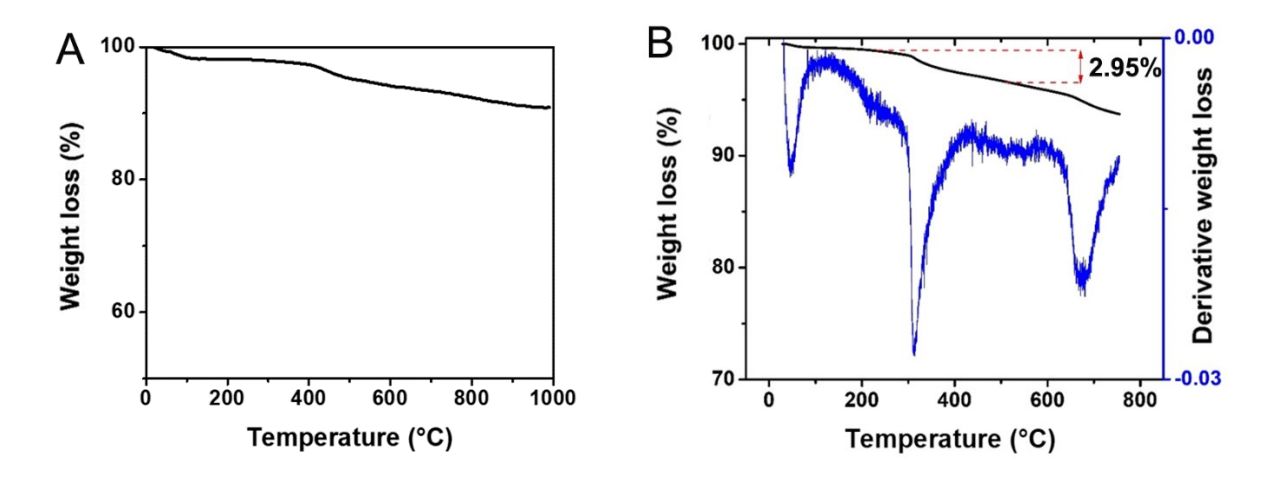


Fig.3. (A) Thermogravimetric analysis of hydrophobized discoids. (B) a zoomed region used to identify the amount of methyl group; the derivative of the weight loss is also shown.

Confocal Raman microscopy/spectroscopy can show the spatial distribution of methyl groups inside discoids. The results of Raman spectroscopy of modified discoids are shown in Figure 4. One can see Raman peaks corresponding to C-H stretching vibrations from methyl groups in the region 2750-3100 cm⁻¹ and CH₃ deformations around 1420 cm⁻¹, Fig4A. (C-Si stretch could also be observed at 620 cm⁻¹ [65].) A strong signal coming from C-H bonds was used to map 3D distribution of C-H stretching vibrations from methyl groups through the volume of the discoids, Fig.4B. One can see that the alkyl modification is well distributed through the volume of the particles.

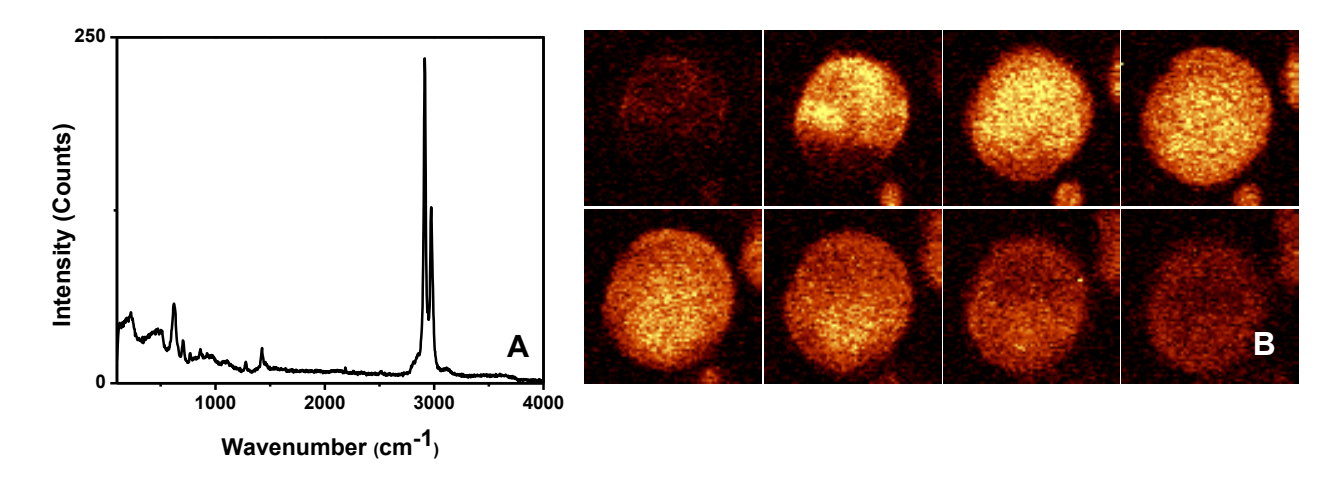


Fig. 4. A) Raman spectra of hydrophobized discoids. B) 8.6 x 8.5 μm² confocal Z-stack Raman images of hydrophobized discoids at 1um intervals. The area under the CH

stretching bands between 2800 and 3100 cm⁻¹ was used to create the maps of the distribution of methyl groups inside the discoid.

The absorption capacity of discoids for various organic compounds was assessed using thermogravimetry. The compounds were absorbed by discoids from a 20% water solution after suspending for 2h. This seems to be a sufficient time to reach the saturation absorption. To check it, we tested the kinetics of absorption. It is rather simple to see with naked eyes for the case of absorption of petroleum standard. For a better visibility, oil was stained with a small amount of rhodamine 6G, red dye. One can see that the oil makes the particles homogeneously pink color within seconds, as shown in a movie (see, the movie in the Supporting information). We further demonstrate it for chloroform and xylene, the materials which have two distinctive sizes of molecules. The results are shown in figure S1 (Supporting information). It can be seen that the absorption of both compounds happens much quicker than the 2 h time used for the absorption studies. Thus, we conclude that the long-time used for stirring allows measuring the saturation value of the absorbed compounds.

The values for saturated capacity for different organic compounds are provided in figure 5. The highest values observed are for ASTM crude oil standard and xylene, which were absorbed up to 120 % of its weight. Based on the measured empty volume per gram of particles, we can conclude that the oil is retained between the particles in this case, not only inside the pores. This is consistent with the previous observations [62].

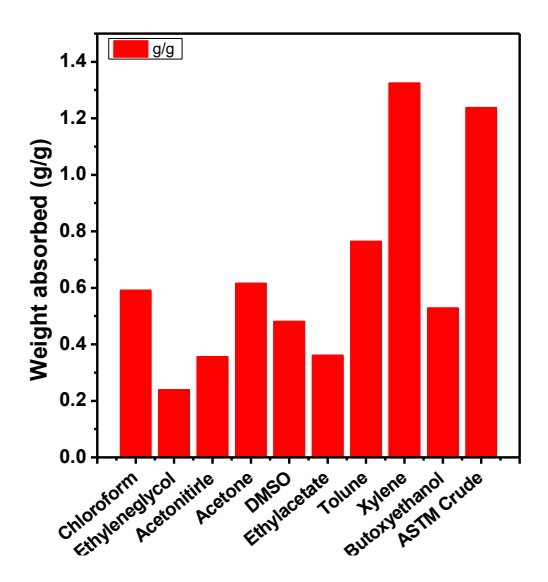


Fig. 5. Amounts of organic compounds absorbed by hydrophobized discoids from a 20% water mixture (in grams of absorbed compound per gram of absorbent material). The compounds are ordered from the smallest molecular size (the most left) to the maximum one (the most right).

To understand the sorption dependence of the components on the size and polarity of molecules, figure 5 presents the results of saturated absorbance for the compounds ordered in the horizontal axis by the size of their molecules. One can see that there is a little dependence of the absorbed amount on the molecular size of the compound. Since the internal surface of discoids is hydrophobic, it would be plausible to expect that this absorbance value correlates with the polarity of the compound if the material were macroscopic. However, in the case of nanoscale cylindrical channels, this effect might be smeared by strong capillary forces, which could suck organic compounds into such pores. Nevertheless, our results showed that the amount of compound absorbed decreases with the increase of the relative polarity. This is shown in figure 6, in which the amount of absorbed compound is plotted against the relative polarity of the compound.

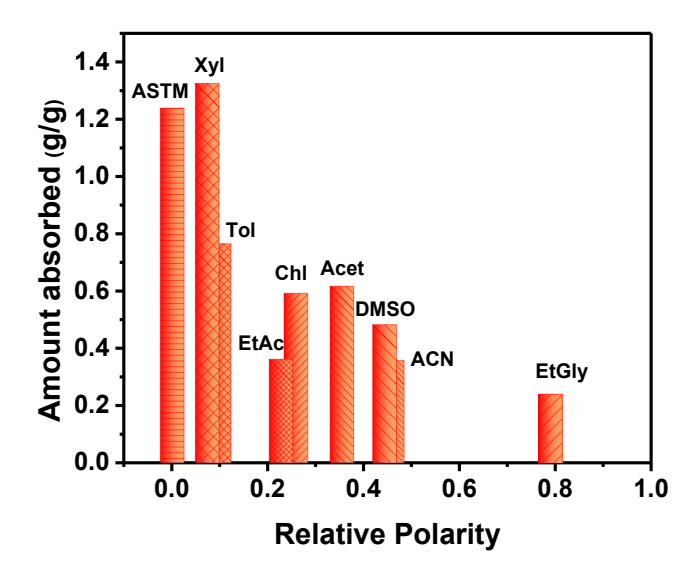


Fig. 6. Amounts of organic compounds absorbed by hydrophobized discoids from a 20% water mixture plotted against the relative polarity of the compound.

It is instrumental to demonstrate that the absorption is driven mainly by the hydrophobic (methyl) groups in discoids. While it is well-known at the macroscale, to the best of the authors' knowledge, it has not been demonstrated for the nanoscale. We demonstrate it using the example of DMSO. Specifically, confocal Raman imaging of DMSO absorbed discoids was used to obtain simultaneous spatial distributions of both hydrophobic methyl groups and DMSO absorbed in a discoid (as previously, the discoid were immersed in DMSO solution for two hours before imaging). The Raman spectrum of such a discoid is shown in Fig.7D. The asymmetric C-H stretching vibrations of methyl groups in the hydrophobic modification can be seen between 2953-2985 cm⁻¹, whereas the peaks indicative of dimethylsulfoxide appear between 3000-3050 cm⁻¹. These are the best discriminators of these two substances (see the extended-scale Raman spectra, Fig.S2 of Supporting information). Because these peaks do not overlap, they were chosen to create the confocal images showing the spatial distribution of the hydrophobic methyl groups and DMSO inside a discoid, Fig.7A,B. Fig.7C shows the colocalization of methyl groups and DMSO. It is built as follows. The red/yellow color of methyl groups shown in Fig.7A is superimposed on the

blue color of DMSO shown in Fig.7C. Homogeneity of the resulted green color indicates the perfect colocalization of hydrophobic methyl groups and DMSO inside the discoid (Fig.7D, right).

It should be noted that the observed strong colocalization of hydrophobic groups and absorbed material is rather nontrivial because of possible strong capillary fact, which would lead to a significant suction force pushing the organic compounds inside the particles. Regretfully, the speed of Raman spectroscopy does not allow us to detect the dynamics of the sorption process. Presumably, the observed colocalization is a result of thermal equilibration, which is reached within the particles during the sorption time and subsequent Raman imaging. This would be in agreement with fast adsorption kinetics reported in [43].

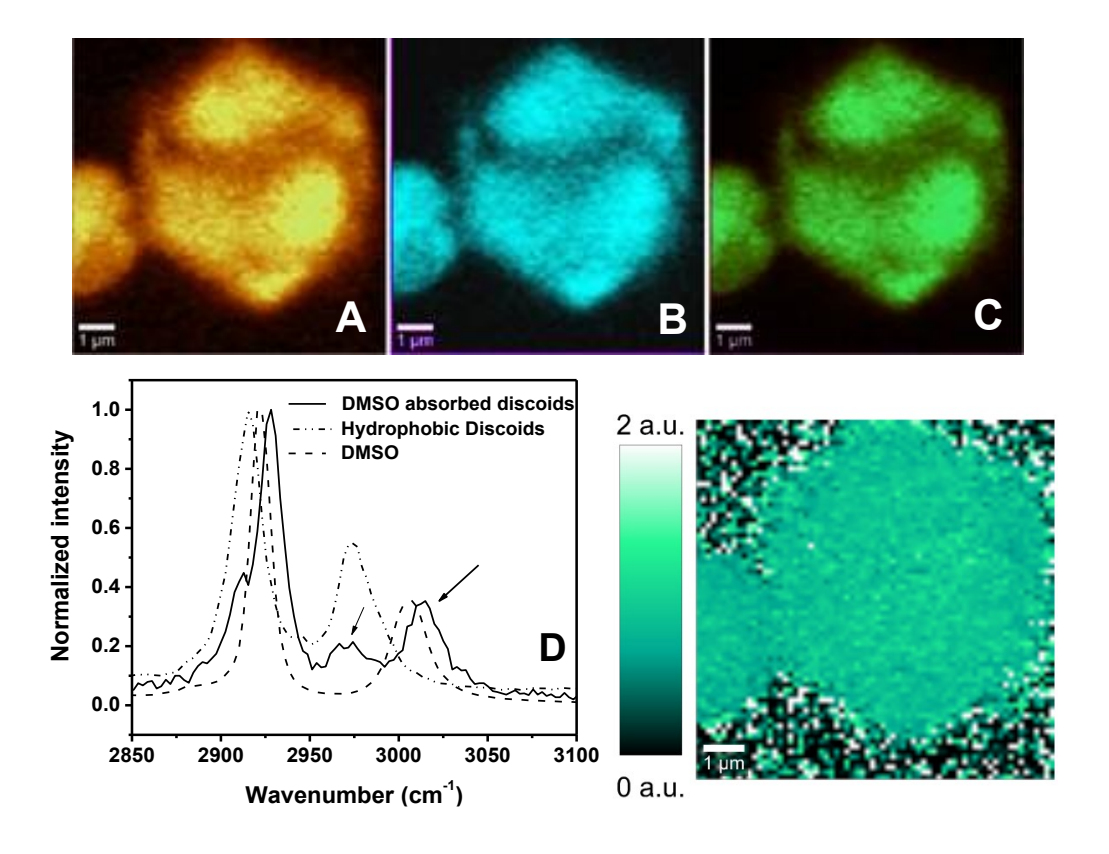


Fig. 7. Colocalization of hydrophobic groups and absorption of dimethylsulfoxide (DMSO). (A-C) Raman confocal images of dimethylsulfoxide absorbed discoids. A) Hydrophobic groups of the modified discoids (asymmetric C-H stretching vibrations of methyl groups have Raman peak at 2953-2985 cm⁻¹), B) DMSO groups (3000-3050 cm⁻¹; intensity scales are the same for both images). C) Co-localized image of hydrophobic

groups A and DMSO B; green color is a result of proportional mixing between red and blue of A and B. (D) Raman spectra of DMSO, hydrophobic discoids, and DMSO absorbed discoids in the region 2850-3100 cm⁻¹; this panel demonstrates the zoom at a particular wavelength range that was used to produce confocal Raman images A and B. The spectral peaks used to obtain images of hydrophobic groups and absorbed DMSO (2980 cm⁻¹ and 3020 cm⁻¹, respectively) are indicated by arrows.

It is useful to demonstrate that the absorbed compounds can be removed from the particles relatively easily. We demonstrate it for the example of the ASTM standard of crude oil. TGA measurements (Fig.S3, Supporting information) show that absorbed oil is removed in a single step under vacuum at 90°C. The amount of absorbed oil removed at different time intervals is plotted in the graph. The amount of oil absorbed was calculated using the percentage weight loss observed in the TGA curve. The results show that about 93% of the oil is removed from the porous silica material by this simple heat treatment. As expected, the number of hydrophobic groups remains unchanged (as seen with the help of Raman spectroscopy, not shown). The number of regenerations of porous silica material should depend on both the particular compound and specific other contaminations in the medium used to separate organics (those can potentially degrade silica matrix differently). Therefore, this part of the study will be done in future works.

At the end, it is instructional to compare the sorption capacity of the described material with the commercially available and other absorbents reported in the literature. It makes sense to separate the absorbents used for the sorption of low polarity water-immiscible materials like crude oil and the absorbance for higher polarity like toluene. The former ones may stick well to the material of relatively large porosity, whereas the latter one requires finer porosity to be captured. The absorption capacity of commercial absorbents expanded perlite and cellulose fiber along with polypropylene fibers were compared in [66]. The performance of these absorbents ranges from 1.8 to 3.5 g/g for various perlite and up to 4.5 g/g for polypropylene. The crude oil absorption capacity of commercial sorbents K-sorb and Spaghetti, along with commercial cotton, is compared in [67]. The reported absorbance capacity was in the range of 0.1 - 0.5 g/g. The most commonly used rubber absorbents used for oil spill recovery were tested in [68], and a capacity of 1 g/g was

observed for petroleum. Thus, the reported here absorbent is comparable to some of the existing ones when used for the absorption of such organic compound as petroleum.

When comparing the sorption of higher polarity organic compounds, such as toluene, nanoporous absorbents are typically used. For example, various absorbents based on activated carbon can effectively absorb 90-200 mg/g of benzene and 100-220 mg/g of toluene [69]. Various mesoporous silica compounds (obtained with the use of organic precursors) were studied for sorption of toluene in [70], in which 270-492 mg/g sorption capacity was reported. The reported here absorbent exceeds this capacity quite substantially (>700 mg/g).

4. Conclusions

Absorptive property of mesoporous silica material is important due to a large number of contaminations of water with oils and various organics, which is dangerous for human health and the environment. Here we demonstrated the ability of inexpensive mesoporous silica material to absorb multiple organic compounds. An unusually high surface area of this material allowed for effective sorption of multiple organic compounds that are treated as common contaminants, chloroform, ethylene glycol, acetonitrile, acetone, dimethylsulfoxide, ethyl acetate, toluene, xylene, 2-butoxyethanol, and ASTM D5307 crude oil standard. We found that absorbance is strongly correlated with the location of hydrophobic groups and inversely proportional to the polarity of organic compounds, whereas there was almost no dependence on the molecular size observed. This information has never been reported for the sorption of organic compounds by nanostructured materials. It can be useful for the development of novel effective absorbents. The ability of silica to be regenerated is also promising because it can decrease the cost of its use and maintenance.

Funding information

The support from the National Science Foundation, grants CBET 1605405 and 1428919 is acknowledged by I.S. Any opinions, findings, and conclusions or recommendations expressed in

this material are those of the author(s) and do not necessarily reflect the views of the National Science Foundation.

Declaration of competing interest

The authors declare that they have no known competing financial interests or personal relationships that could have appeared to influence the work reported in this paper.

Appendix A. Supplementary data

The following is the supplementary data to this article:

- Time dependence of the absorption of chloroform and toluene from water by hydrophobized discoids (Fig.S1);
- An extended-scale Raman spectra of DMSO, hydrophobic discoids, and DMSO absorbed discoids (Fig.S2);
- The removal rate of adsorbed oil under vacuum at 90 °C (Fig.S3).
- Calculation of density of methyl groups
- Movie: Absorption of ASTM standard crude oil by nanoporous silica material. (The transparent crude oil standard is stained with rhodamine dye for visibility.)

References

- [1] T.-L. Chen, C.-Y. Huang, Y.-T. Xie, Y.-Y. Chiang, Y.-M. Chen, H.-Y. Hsueh, Bioinspired Durable Superhydrophobic Surface from a Hierarchically Wrinkled Nanoporous Polymer, ACS Applied Materials & Interfaces, 11 (2019) 40875-40885.
- [2] Y. Zhang, S. Wei, F. Liu, Y. Du, S. Liu, Y. Ji, T. Yokoi, T. Tatsumi, F.-S. Xiao, Superhydrophobic nanoporous polymers as efficient adsorbents for organic compounds, Nano Today, 4 (2009) 135-142.

- [3] E. Scholten, L. Bromberg, G.C. Rutledge, T.A. Hatton, Electrospun Polyurethane Fibers for Absorption of Volatile Organic Compounds from Air, ACS Applied Materials & Interfaces, 3 (2011) 3902-3909.
- [4] J. Wu, N. Wang, L. Wang, H. Dong, Y. Zhao, L. Jiang, Electrospun Porous Structure Fibrous Film with High Oil Adsorption Capacity, ACS Applied Materials & Interfaces, 4 (2012) 3207-3212.
- [5] M. Williams, N.J. Warren, L.A. Fielding, S.P. Armes, P. Verstraete, J. Smets, Preparation of Double Emulsions using Hybrid Polymer/Silica Particles: New Pickering Emulsifiers with Adjustable Surface Wettability, ACS Applied Materials & Interfaces, 6 (2014) 20919-20927.
- [6] D. Yang, J. Li, Y. Xu, D. Wu, Y. Sun, H. Zhu, F. Deng, Direct formation of hydrophobic silica-based micro/mesoporous hybrids from polymethylhydrosiloxane and tetraethoxysilane, Microporous and Mesoporous Materials, 95 (2006) 180-186.
- [7] P. Lopez-Aranguren, J. Saurina, L.F. Vega, C. Domingo, Sorption of tryalkoxysilane in low-cost porous silicates using a supercritical CO2 method, Microporous and Mesoporous Materials, 148 (2012) 15-24.
- [8] Ł. Osuchowski, B. Szczęśniak, J. Choma, M. Jaroniec, High benzene adsorption capacity of micro-mesoporous carbon spheres prepared from XAD-4 resin beads with pores protected effectively by silica, Journal of Materials Science, 54 (2019) 13892-13900.
- [9] V. Janout, S.B. Myers, R.A. Register, S.L. Regen, Self-Cleaning Resins, Journal of the American Chemical Society, 129 (2007) 5756-5759.
- [10] Y. Yang, Y. Deng, Z. Tong, C. Wang, Multifunctional foams derived from poly(melamine formaldehyde) as recyclable oil absorbents, Journal of Materials Chemistry A, 2 (2014) 9994-9999.
- [11] Z. Zhang, G. Sèbe, D. Rentsch, T. Zimmermann, P. Tingaut, Ultralightweight and Flexible Silylated Nanocellulose Sponges for the Selective Removal of Oil from Water, Chemistry of Materials, 26 (2014) 2659-2668.
- [12] C. Feng, Z. Yi, F. She, W. Gao, Z. Peng, C.J. Garvey, L.F. Dumée, L. Kong, Superhydrophobic and Superoleophilic Micro-Wrinkled Reduced Graphene Oxide as a Highly Portable and Recyclable Oil Sorbent, ACS Applied Materials & Interfaces, 8 (2016) 9977-9985.

- [13] V.V.C. Lima, F.B. Dalla Nora, E.C. Peres, G.S. Reis, É.C. Lima, M.L.S. Oliveira, G.L. Dotto, Synthesis and characterization of biopolymers functionalized with APTES (3–aminopropyltriethoxysilane) for the adsorption of sunset yellow dye, Journal of Environmental Chemical Engineering, 7 (2019) 103410.
- [14] C. Solisio, A. Lodi, A. Converti, M.D. Borghi, Removal of exhausted oils by adsorption on mixed Ca and Mg oxides, Water Research, 36 (2002) 899-904.
- [15] S.-Y. Jeong, H. Jin, J.-M. Lee, D.-J. Yim, Adsorption on Ti- and Al-containing mesoporous materials prepared from fluorosilicon, Microporous and Mesoporous Materials, 44-45 (2001) 717-723.
- [16] V. Rajaković-Ognjanović, G. Aleksić, L. Rajaković, Governing factors for motor oil removal from water with different sorption materials, Journal of Hazardous Materials, 154 (2008) 558-563.
- [17] D. Wang, T. Silbaugh, R. Pfeffer, Y.S. Lin, Removal of emulsified oil from water by inverse fluidization of hydrophobic aerogels, Powder Technology, 203 (2010) 298-309.
- [18] D.B. Mahadik, K.-Y. Lee, R.V. Ghorpade, H.-H. Park, Superhydrophobic and Compressible Silica-polyHIPE Covalently Bonded Porous Networks via Emulsion Templating for Oil Spill Cleanup and Recovery, Scientific Reports, 8 (2018) 16783.
- [19] B. Vivek, E. Prasad, Self-Assembly-Directed Aerogel and Membrane Formation from a Magnetic Composite: An Approach to Developing Multifunctional Materials, ACS Applied Materials & Interfaces, 9 (2017) 7619-7628.
- [20] C. Duan, T. Zhu, J. Guo, Z. Wang, X. Liu, H. Wang, X. Xu, Y. Jin, N. Zhao, J. Xu, Smart Enrichment and Facile Separation of Oil from Emulsions and Mixtures by Superhydrophobic/Superoleophilic Particles, ACS Applied Materials & Interfaces, 7 (2015) 10475-10481.
- [21] S. Yu, H. Tan, J. Wang, X. Liu, K. Zhou, High Porosity Supermacroporous Polystyrene Materials with Excellent Oil–Water Separation and Gas Permeability Properties, ACS Applied Materials & Interfaces, 7 (2015) 6745-6753.
- [22] S. Qiu, M. Xue, G. Zhu, Metal–organic framework membranes: from synthesis to separation application, Chemical Society Reviews, 43 (2014) 6116-6140.

- [23] D. Wang, E. McLaughlin, R. Pfeffer, Y.S. Lin, Adsorption of oils from pure liquid and oil—water emulsion on hydrophobic silica aerogels, Separation and Purification Technology, 99 (2012) 28-35.
- [24] A. Venkateswara Rao, N.D. Hegde, H. Hirashima, Absorption and desorption of organic liquids in elastic superhydrophobic silica aerogels, Journal of Colloid and Interface Science, 305 (2007) 124-132.
- [25] J.G. Reynolds, P.R. Coronado, L.W. Hrubesh, Hydrophobic aerogels for oil-spill clean up synthesis and characterization, Journal of Non-Crystalline Solids, 292 (2001) 127-137.
- [26] H. Hu, Z. Zhao, Y. Gogotsi, J. Qiu, Compressible Carbon Nanotube–Graphene Hybrid Aerogels with Superhydrophobicity and Superoleophilicity for Oil Sorption, Environmental Science & Technology Letters, 1 (2014) 214-220.
- [27] Q. Ma, H. Cheng, A.G. Fane, R. Wang, H. Zhang, Recent Development of Advanced Materials with Special Wettability for Selective Oil/Water Separation, Small, 12 (2016) 2186-2202.
- [28] A. Walcarius, Mesoporous Materials-Based Electrochemical Sensors, Electroanalysis, 27 (2015) 1303-1340.
- [29] V. Fathi Vavsari, G. Mohammadi Ziarani, A. Badiei, The role of SBA-15 in drug delivery, RSC Advances, 5 (2015) 91686-91707.
- [30] S.R.a.F.Y.Y. Joshua Gan, A Review on Improvement of LED Light Extraction Efficiency through a Micro Repeating Structure, Reviews in advanced material science, 42 (2015) 92-101.
- [31] N. Sharma, H. Ojha, A. Bharadwaj, D.P. Pathak, R.K. Sharma, Preparation and catalytic applications of nanomaterials: a review, RSC Advances, 5 (2015) 53381-53403.
- [32] T. Cheng, Q. Zhao, D. Zhang, G. Liu, Transition-metal-functionalized ordered mesoporous silicas: an overview of sustainable chiral catalysts for enantioselective transformations, Green Chemistry, 17 (2015) 2100-2122.
- [33] D.J. Lunter, Evaluation of mesoporous silica particles as drug carriers in hydrogels, Pharmaceutical Development and Technology, 23 (2018) 826-831.
- [34] P. Van Der Voort, D. Esquivel, E. De Canck, F. Goethals, I. Van Driessche, F.J. Romero-Salguero, Periodic Mesoporous Organosilicas: from simple to complex bridges; a

- comprehensive overview of functions, morphologies and applications, Chemical Society Reviews, 42 (2013) 3913-3955.
- [35] G.J.A.A. Soler-Illia, O. Azzaroni, Multifunctional hybrids by combining ordered mesoporous materials and macromolecular building blocks, Chemical Society Reviews, 40 (2011) 1107-1150.
- [36] B. Sun, G. Zhou, H. Zhang, Synthesis, functionalization, and applications of morphology-controllable silica-based nanostructures: A review, Progress in Solid State Chemistry, 44 (2016) 1-19.
- [37] A. Sayari, S. Hamoudi, Periodic Mesoporous Silica-Based Organic-Inorganic Nanocomposite Materials, Chemistry of Materials, 13 (2001) 3151-3168.
- [38] H. Sepehrian, M. Ghannadi-Maragheh, S. Waqif-Husain, R. Yavari, A.R. Khanchi, Sorption studies of radionuclides on a modified mesoporous cerium(IV) silicate, J Radioanal Nucl Ch, 275 (2008) 145-153.
- [39] M. Zhou, H. Zhang, L. Xiong, Z. He, A. Zhong, T. Wang, Y. Xu, K. Huang, Synthesis of magnetic microporous organic nanotube networks for adsorption application, RSC Advances, 6 (2016) 87745-87752.
- [40] R. Kishor, A.K. Ghoshal, High molecular weight polyethyleneimine functionalized three dimensional mesoporous silica for regenerable CO2 separation, Chemical Engineering Journal, 300 (2016) 236-244.
- [41] M.J. Al-Marri, M.M. Khader, M. Tawfik, G. Qi, E.P. Giannelis, CO2 Sorption Kinetics of Scaled-Up Polyethylenimine-Functionalized Mesoporous Silica Sorbent, Langmuir, 31 (2015) 3569-3576.
- [42] H. Wang, T. Wang, L. Han, M. Tang, J. Zhong, W. Huang, R. Chen, VOC adsorption and desorption behavior of hydrophobic, functionalized SBA-15, Journal of Materials Research, 31 (2016) 516-525.
- [43] J. Liu, X. Feng, G.E. Fryxell, L.-Q. Wang, A.Y. Kim, M. Gong, Hybrid Mesoporous Materials with Functionalized Monolayers, Advanced Materials, 10 (1998) 161-165.
- [44] Y. Liu, Z. Li, X. Yang, Y. Xing, C. Tsai, Q. Yang, Z. Wang, R.T. Yang, Performance of mesoporous silicas (MCM-41 and SBA-15) and carbon (CMK-3) in the removal of gasphase naphthalene: adsorption capacity, rate and regenerability, RSC Advances, 6 (2016) 21193-21203.

- [45] I. Batonneau-Gener, A. Yonli, A. Trouvé, S. Mignard, M. Guidotti, M. Sgobba, Tailoring the Hydrophobic Character of Mesoporous Silica by Silylation for VOC Removal, Separation Science and Technology, 45 (2010) 768-775.
- [46] Q. Hu, J.J. Li, Z.P. Hao, L.D. Li, S.Z. Qiao, Dynamic adsorption of volatile organic compounds on organofunctionalized SBA-15 materials, Chemical Engineering Journal, 149 (2009) 281-288.
- [47] B. Dou, Q. Hu, J. Li, S. Qiao, Z. Hao, Adsorption performance of VOCs in ordered mesoporous silicas with different pore structures and surface chemistry, Journal of Hazardous Materials, 186 (2011) 1615-1624.
- [48] X.S. Zhao, G.Q. Lu, Modification of MCM-41 by Surface Silylation with Trimethylchlorosilane and Adsorption Study, The Journal of Physical Chemistry B, 102 (1998) 1556-1561.
- [49] J.A.S. Costa, R.A. de Jesus, C.M.P. da Silva, L.P.C. Romão, Efficient adsorption of a mixture of polycyclic aromatic hydrocarbons (PAHs) by Si–MCM–41 mesoporous molecular sieve, Powder Technology, 308 (2017) 434-441.
- [50] R.S. Araújo, D.C.S. Azevedo, C.L. Cavalcante, A. Jiménez-López, E. Rodríguez-Castellón, Adsorption of polycyclic aromatic hydrocarbons (PAHs) from isooctane solutions by mesoporous molecular sieves: Influence of the surface acidity, Microporous and Mesoporous Materials, 108 (2008) 213-222.
- [51] S.K. Toor, J.P. Kushwaha, V.K. Sangal, Adsorptive interaction of 4-aminobiphenyl with mesoporous MCM-41, Physics and Chemistry of Liquids, 57 (2019) 720-732.
- [52] M. Sadeghi, S. Yekta, H. Ghaedi, Synthesis and application of Pb-MCM-41/ZnNiO2 as a novel mesoporous nanocomposite adsorbent for the decontamination of chloroethyl phenyl sulfide (CEPS), Applied Surface Science, 400 (2017) 471-480.
- [53] Y. Guo, W. Huang, B. Chen, Y. Zhao, D. Liu, Y. Sun, B. Gong, Removal of tetracycline from aqueous solution by MCM-41-zeolite A loaded nano zero valent iron: Synthesis, characteristic, adsorption performance and mechanism, Journal of Hazardous Materials, 339 (2017) 22-32.
- [54] D.O. Santos, M. de Lourdes Nascimento Santos, J.A.S. Costa, R.A. de Jesus, S. Navickiene, E.M. Sussuchi, M.E. de Mesquita, Investigating the potential of functionalized MCM-41 on

- adsorption of Remazol Red dye, Environmental Science and Pollution Research, 20 (2013) 5028-5035.
- [55] S.O. Akpotu, B. Moodley, Application of as-synthesised MCM-41 and MCM-41 wrapped with reduced graphene oxide/graphene oxide in the remediation of acetaminophen and aspirin from aqueous system, Journal of Environmental Management, 209 (2018) 205-215.
- [56] R. Li, L. Zhang, P. Wang, Rational design of nanomaterials for water treatment, Nanoscale, 7 (2015) 17167-17194.
- [57] C. Cheng, X. Tan, D. Lu, L. Wang, T. Sen, J. Lei, A.M. El-Toni, J. Zhang, F. Zhang, D. Zhao, Carbon-Dot-Sensitized, Nitrogen-Doped TiO2 in Mesoporous Silica for Water Decontamination through Nonhydrophobic Enrichment–Degradation Mode, Chemistry A European Journal, 21 (2015) 17944-17950.
- [58] S.P. Naik, I. Sokolov, Synthesis of mesoporous silica fibers and discoids endowed with circular pore architecture using disodium trioxosilicate as silica source, Microporous and Mesoporous Materials, 116 (2008) 581-585.
- [59] D.O. Volkov, E.-B. Cho, I. Sokolov, Synthesis of ultrabright nanoporous fluorescent silica discoids using an inorganic silica precursor, Nanoscale, 3 (2011) 2036-2043.
- [60] I. Sokolov, Y.Y. Kievsky, J.M. Kaszpurenko, Self-Assembly of Ultrabright Fluorescent Silica Particles, Small, 3 (2007) 419-423.
- [61] D. Zadaka-Amir, N. Bleiman, Y.G. Mishael, Sepiolite as an effective natural porous adsorbent for surface oil-spill, Microporous and Mesoporous Materials, 169 (2013) 153-159.
- [62] C. Gérardin, J. Reboul, M. Bonne, B. Lebeau, Ecodesign of ordered mesoporous silica materials, Chemical Society Reviews, 42 (2013) 4217-4255.
- [63] V. Kalaparthi, S. Palantavida, N.E. Mordvinova, O.I. Lebedev, I. Sokolov, Self-assembly of multi-hierarchically structured spongy mesoporous silica particles and mechanism of their formation, Journal of Colloid and Interface Science, 491 (2017) 133-140.
- [64] I. Sokolov, V. Kalaparthi, D.O. Volkov, S. Palantavida, N.E. Mordvinova, O.I. Lebedev, J. Owens, Control and formation mechanism of extended nanochannel geometry in colloidal mesoporous silica particles, Physical Chemistry Chemical Physics, 19 (2017) 1115-1121.

- [65] V. Kalaparthi, S. Palantavida, I. Sokolov, The nature of ultrabrightness of nanoporous fluorescent particles with physically encapsulated fluorescent dyes, Journal of Materials Chemistry C, 4 (2016) 2197-2210.
- [66] C. Teas, S. Kalligeros, F. Zanikos, S. Stournas, E. Lois, G. Anastopoulos, Investigation of the effectiveness of absorbent materials in oil spills clean up, Desalination, 140 (2001) 259-264.
- [67] R. Pagnucco, M.L. Phillips, Comparative effectiveness of natural by-products and synthetic sorbents in oil spill booms, J Environ Manage, 225 (2018) 10-16.
- [68] S. Venkatanarasimhan, D. Raghavachari, Epoxidized natural rubber-magnetite nanocomposites for oil spill recovery, J Mater Chem A, 1 (2013) 868-876.
- [69] N. Wibowo, L. Setyadhi, D. Wibowo, J. Setiawan, S. Ismadji, Adsorption of benzene and toluene from aqueous solutions onto activated carbon and its acid and heat treated forms: Influence of surface chemistry on adsorption, Journal of Hazardous Materials, 146 (2007) 237-242.
- [70] A. Trouve, I. Batonneau-Gener, S. Valange, M. Bonne, S. Mignard, Tuning the hydrophobicity of mesoporous silica materials for the adsorption of organic pollutant in aqueous solution, Journal of Hazardous Materials, 201 (2012) 107-114.